Progress In Electromagnetics Research, PIER 86, 111–134, 2008

A SYMMETRY-BASED FORMALISM FOR THE ELECTRODYNAMICS OF NANOTUBES

S. M. Mikki and A. A. Kishk

Center of Applied Electromagnetic Systems Research
Department of Electrical Engineering
University of Mississippi
University, MS 38677, USA

Abstract—In this paper, a general symmetry-based approach to the electrodynamics of a class of low-dimensional structures, carbon nanotubes, is proposed. The contribution of the microscopic configuration is handled using the symmetry group of the structure under consideration. An explicit form of the electromagnetic field is derived starting from a general nonlocal linear susceptibility model expressed as a low-dimensional phenomenological response function. The general form of the field obtained is used to devise new theoretical insights by providing a framework for the computation of the nanotube Green's functions.

1. INTRODUCTION

There is an increasing interest in employing applications from nanotechnology to develop new generation of materials and devices that can handle the growing demands of industry [1]. Of special importance is a class of low-dimensional structures called carbon nanotubes (CNT), which were discovered in 1991 by Iijima [1–3]. Since then, they have attracted the attention of both physicists and engineers who investigated extensively the possibility of using CNTs for various applications, ranging from mechanical shielding to nano-waveguide and transistors [5, 6]. One of the most attractive features in CNTs is their ability to function in either metallic or semi-conducting modes, depending on how the original graphite sheet is rolled to form the tube [6]. Such plethora of advantages suggest that CNTs may become the vital device of future nono-electronics when reaching the fundamental size limit of the current silicon micro-electronics industry.

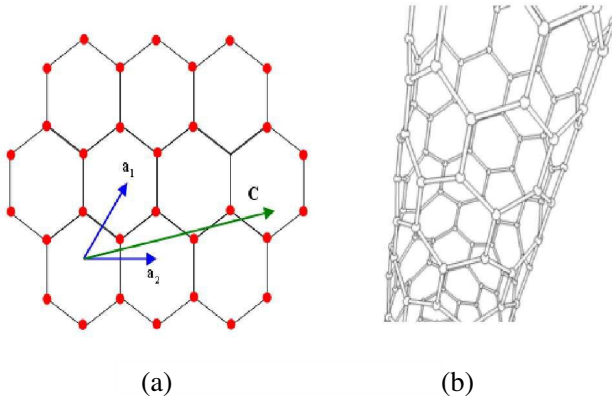

Figure 1. (a) Graphene sheet used in forming CNTs (The dots illustrate the carbon atoms positions). (b) Geometry of a single-wall carbon nanotube (SWCNT).

Our goal in this paper is to show systematically how nontrivial differences between conventional and nano-electromagnetics can be accounted for once the conceptual corrections of the nanoscale problem are taken into consideration. In order to keep the problem at the practical level, a concrete example, carbon nanotubes, has been chosen to function as a vehicle for the illustration of the various theoretical ideas we are proposing for nanoelectromagnetics. Those nanotubes demonstrate nicely several peculiarities unique in nanoscale problems. First, they are, obviously, microscopic structures, leading to the fact that a direct conventional electrodynamic approach will probably fail to account for the full nature of their physics. Second, since atoms in carbon nanotubes are arranged geometrically in a cylindrical fashion, with very high aspect ration, they serve as toy models illustrating the electrodynamics as taking place in a lower-dimensional space, in this case 1-D. Such interpretation may help in suggesting, at least theoretically, new ways of viewing Maxwell's equations, different from the bulk matter approach of conventional macroscopic electrodynamics. Third, as we mentioned above, carbon nanotubes are very promising stable microscopic structures that have found various mechanical and electrical applications and are expected to play important role in future nano-electronics and other industries. Therefore, the task of employing them in the demonstration of the peculiarities of nanoscale electromagnetics is advantageous by itself, since many of the results derived throughout can be easily adapted in future work.

2. GENERAL CONSIDERATIONS FOR THEORETICAL NANO-ELECTROMAGNETICS

The conventional approach to the discourse of engineering, macroscopic electromagnetics is summarized in Figure 2. The threefold process constituting the core of this discourse can be explicated in the the following way.

(i) Define an excitation, a macroscopic concentration of electric charge and current $\mathbf{J}_s$ and/or equivalent magnetic currents $\mathbf{M}_s$.

(ii) Define a macroscopic boundary Ω separating various regions in space, each modeled unambiguously by an effective dielectric and magnetic permeability.

(iii) Solve Maxwell's equations by formulating them as a boundary-value problem in mathematical physics. Step 1 above provides the source (driving) term in the partial differential equations, while Step 2 specifies the boundary condition imposed on those equations. The outcome of this solution process is the electromagnetic fields everywhere, $\mathbf{E}$ and $\mathbf{H}$.

This formulation is complete in the sense that once the constitutive relations $\mathbf{D} = \varepsilon\mathbf{E}$ and $\mathbf{B} = \mu\mathbf{H}$ are known, Maxwell's equations can be solved to produce the unique set of fields satisfying the boundary condition of the problem. Due to this mathematical completeness, engineering electromagnetics has progressed throughout most of the previous century with minimum contact with other branches in physics.

However, this autonomy has been possible only because the problem is *macroscopic*. That is, the devices used to measure the electromagnetic fields already perform an averaging process, which washes out the fast components of the fields. This leads to the ability to

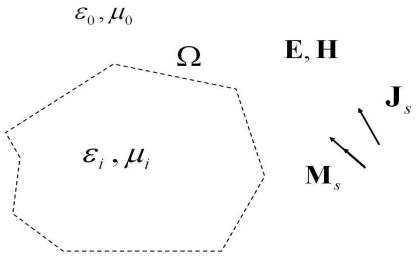

Figure 2. A general illustration of the formulation of macroscopic electromagnetic problems.

replace the inherently discontinues structure of matter by the smooth, continuous representation of the boundary Ω in Figure 2. Once the scale of the electromagnetic problem is pushed downward toward the nano-world, the discontinuity of matter becomes much more manifest. This leads to important corrections to be introduced to conventional (macroscopic) electromagnetics. Our claim is that those corrections are not just quantitative, in the sense that the numerical values of the effective medium functions ε and μ are going to change, but, most importantly, there are fundamental *conceptual* modifications that must be taken directly into considerations in order to understand why the problem at the nanoscale level presents something new to the electromagnetic community.

We mention two corrections to be taken into account for a successful description of the electrodynamics at the nanoscale level.

(i) The size effects (e.g., quantum confinement.)

(ii) The nonlocal effects (e.g., spatial dispersion.)

The size effects relate to the quantum mechanical phenomena of confinement. Since, according to the de Broglie's hypothesis, each particle has a wave associated with it, electrons (like photons) existing in very small dimensions will undergo resonator-type quantization effects, which are due to imposing the boundary condition of the spatial structure on the wavefunction. This usually results in new behavior that is not present in the original bulk material response functions.

The nonlocal effects (spatial dispersion) will be emphasized in this paper by demonstrating how the microscopic symmetry group can be used to take into consideration the higher-order Floquet modes.

One has always to remember that there is nothing orthodox in macroscopic Maxwell's equations. The true fundamental physical process is the microscopic equations of the fields *and* the mechanical models used to describe matter. Macroscopic Maxwell's equations are an *effective*-field theory, the outcome of combining these two aspects of reality, field and matter, as is shown in Figure 3. In other words, the electromagnetic process in material media can be visualized as a *coupled mode* of both radiation and matter. This picture applies equally to both bulk material electromagnetics and nanoscale lower-dimensional structures. However, the latter has the additional peculiarity of the so-called size effects of the lower scale. The treatment of the boundary of a lower-dimensional structure is tricky because there is no unique natural interface between different domains. The choice of the boundary condition depends on the way we decide to handle the *mechanical* problem at the aforementioned interface between different media [24].

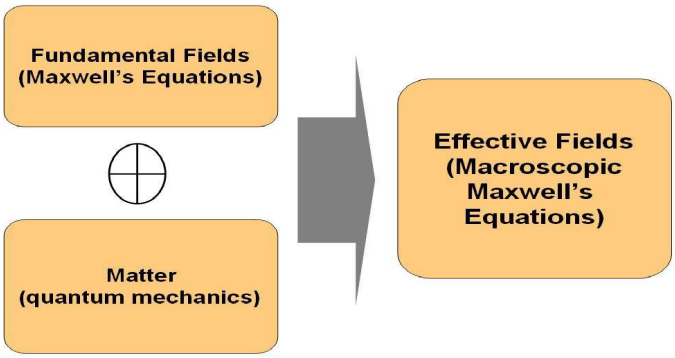

Figure 3. The anatomy of an effective-field electromagnetic theory.

We turn now to the important issue of averaging the fields and the role of quantum mechanics. The microscopic electric source consists of charged particles. Therefore, we can mathematically express this distribution in the following way

$$\rho^{\text{mic}}(\mathbf{r},t) = \sum_i q_i \delta\left[\mathbf{r} - \mathbf{r}_i(t)\right] \tag{1}$$

and

$$\mathbf{j}^{\text{mic}}(\mathbf{r},t) = \sum_i q_i \dot{\mathbf{r}}_i \delta\left[\mathbf{r} - \mathbf{r}_i(t)\right], \tag{2}$$

where $\mathbf{r}_i$ is the position vector if the ith charge q_i. The microscopic Maxwell's equations govern how these sources will generate a dynamics fields $\mathbf{e}$ and $\mathbf{h}$ in the space between the particles. However, the motion of a material particle is not a pure electromagnetic phenomena, but rather a mechanical process that must be described ultimately using quantum mechanics. This mechanics tells us something about the position appearing in (1) and the velocity appearing in (2): They can not be *both* determined with *arbitrary* accuracy, which is the content of Heisenberg's uncertainty relation. The more precise becomes the position, the more uncertain is the velocity (and vice versa.) Therefore, we can not know "exactly" both the charge and the current density. This leads to the problem of stochastic fluctuations, which is an inherently quantum phenomena, leading to the necessity of replacing the classical fields and variables by operators associated with statistical distributions.

Figure 4 illustrates the previous discussion. The fluctuations in the field emphasized there are the *statistical* fluctuations, not the fast-varying components of the fields, which are ultimately due to the

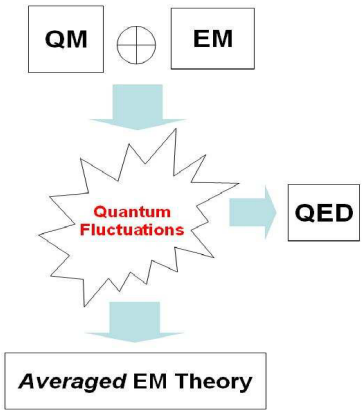

Figure 4. Quantum electrodynamic results from the effort to treat consistently the fluctuations in the electromagnetic fields resulting from talking into account the microscopic mechanical motion of the particles comprising the electric sources. The "averaged EM theory" here is a theory in which the fields variables are averaged only statistically over the ensemble of the quantum mechanically possible state.

nonlocality of the medium. It is important to distinguish between these two types of fluctuations. If a crude averaging procedure is applied to transform the microscopic fields $\mathbf{e}$ and $\mathbf{h}$ to $\mathbf{E}$ and $\mathbf{H}$, respectively, then all information about the microscopic structure will probably be lost. Clearly, for nanoscale device applications we *do* want to retain those non-statistical microscopic information, which are reflected in the high-order Floquet modes, which reflects in turn the spatial structure of the device under consideration. Therefore, we only average the fields statistically, i.e., using the Shrödinger wavefunction as a probability density function. The averaged field theory in Figure 4 refers then only to statistically averaged theory.

Aside from these general consideration, we will not perform any quantum electrodynamics calculations in this paper. The approach is semi-classical in the sense that the fields are going to be treated as classical variables.

3. STRUCTURE OF CARBON NANOTUBES

In this section, we provide a compact description of the structural properties of CNTs using the language of the associated symmetry group. The details of the symmetry operations will be used in the

remaining parts of this chapter to find the specific mathematical form of the eigenmodes appearing in the dielectric tensor of the nanotube. The crux of our approach is that the symmetry group will determine the boundary conditions of the problem [7]. These conditions can not be derived form the Hamiltonian of the CNT but should be obtained through an independent approach.

Figure 1(a) illustrates the honeycomb lattice structure of graphene (graphene is defined as a 2D layer of graphite). The unit cell is specified by two atoms located at the positions $1/3\,(\mathbf{a}_1 + \mathbf{a}_2)$ and $2/3\,(\mathbf{a}_1 + \mathbf{a}_2)$, where $\mathbf{a}_1$ and $\mathbf{a}_2$ are two unit vectors defining the lattice constants and $|\mathbf{a}_1| = |\mathbf{a}_2| = a_0 = 0.2461\,\mathrm{nm}$. The CNT is formed by rolling this sheet such that the circumference of the tube coincides with the *chiral vector* $\mathbf{c} = m\,\mathbf{a}_1 + n\,\mathbf{a}_2$. Here m and n are two integers that completely determine the structure and the properties of the CNT. If only one layer is used to form the tube, the resulting structure is called *single-wall* CNT (SWCNT). Alternatively, if the tube consists of several concentric cylinders, we call it *multi-wall* CNT (MWCNT). The chiral angle θ is defined as the angle between the chiral vector $\mathbf{c}$ and $\mathbf{a}_1$. The radius of the CNT is given by

$$b = \frac{|\mathbf{c}|}{2\pi} = \frac{a_0}{2\pi}\sqrt{m^2 + mn + n^2}. \tag{3}$$

The first symmetry group for the CNT can be derived by writing $\mathbf{c} = N\,[(m/N)\,\mathbf{a}_1 + (n/N)\,\mathbf{a}_2] = N\,\mathbf{c}'$, where N is the greatest common divider of m and n. It is obvious that a rotation around the tube axis by $2\pi/N$ will preserve the original structure. Equivalently, we say that each CNT possess the symmetry operation $\mathbf{C}_N$.

Through knowledge of other symmetry operations, to be discussed in a moment, it is possible by following the original work of White et al. [17] to show that the entire tube can be constructed starting from two-atom unit cell and the chiral vector. The first atom in the unit cell will be mapped to an arbitrary location in the circumference of the CNT, call it A. The second atom will be mapped to other location B obtained by rotating the first point by an angle $\gamma = 2\pi\,(\mathbf{a}_1 + \mathbf{a}_2)\cdot\mathbf{c}/3\,|\mathbf{c}|^2$ and then translating the resulting point along the tube axis by a distance $d = |(\mathbf{a}_1 + \mathbf{a}_2)\times\mathbf{c}|/3\,|\mathbf{c}|^2$. The two points obtained now can be used, together with the symmetry operation $\mathbf{C}_N$, to generate other $2(N-1)$ points by successive rotations around the tube axis by the angle $2\pi/N$. That is, atom A, together with $\mathbf{C}_N$, will generate other $N-1$ atoms. Atom B, again together with $\mathbf{C}_N$, will generate other set of $N-1$ atoms. Therefore, the total is $2\,(N-1) + N = 2N$ atoms. This set is called the *basic helical motif* of the CNT [17]. However, to complete the tube we need to use a *screw operator*, defined in [17], which is

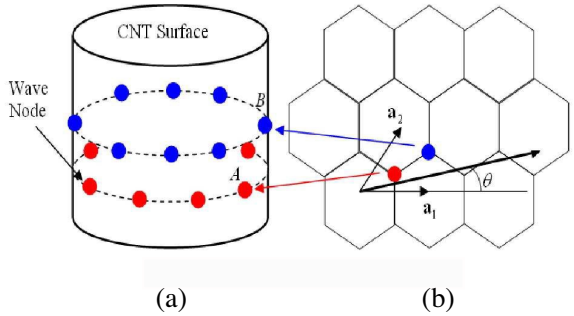

Figure 5. (a) Illustration of two atomic circles in the translational unit cell of a SWCNT. Each circle corresponds to the symmetry operation $\mathbf{C}_N$. (b) The honeycomb lattice structure of graphene. The dots represent the arbitrary first two-atom unit cell.

denoted here by $\mathbf{T}_h^{\zeta}$. Its action on a specific point consists of rotation around the tube axis by an angle ζ and then translation along the tube axis by a distance h. Therefore, the screw operation is neither pure rotation nor pure translation, but a combination of both of them. A procedure for finding ζ and h can be found in [17] and explicit closed form expressions in terms of Euler function are available as follow [18]

$$q = 2\frac{m^2 + mn + n^2}{NR}, \tag{4}$$

$$\xi = \frac{q}{N}\mathrm{Fr}\left[\frac{N}{qR}\left(3 - 2\frac{m-n}{m}\right) + \frac{N}{m}\left(\frac{m-n}{N}\right)^{\mathrm{E}(m/N)-1}\right], \tag{5}$$

$$\zeta = \frac{2\pi}{q}\xi, h = \frac{N}{\xi}a, \tag{6}$$

where $\mathrm{Fr}\,[x] = x - [x]$ gives the fractional part of the rational number x and $\mathrm{E}\,(v)$ is the Euler function giving the co-primes less than v (a is defined in (8)). By repeated application of the screw operator $\mathbf{T}_h^{\zeta}$ on the basic helical motif, the entire tube can be reconstructed [17]. Therefore, the two-atom unit cell that we started with is enough to determine the full structure of the CNT.

It remains to present the translational symmetry of the CNT. Depending on the chirality, each CNT will have a characteristic length a along its axis. Translations of multiples of a will leave the tube

unchanged. This periodicity in the axial direction can be given by [18]

$$N_1 = -\frac{2n+m}{N\mathcal{R}}, N_2 = \frac{2m+n}{N\mathcal{R}}, \tag{7}$$

$$\mathbf{a} = N_1\mathbf{a}_1 + N_2\mathbf{a}_2, a = |\mathbf{a}| = \frac{\sqrt{3\left(m^2+mn+n^2\right)}}{N\mathcal{R}}a_0, \tag{8}$$

$$N_c = \frac{2\left(m^2+mn+n^2\right)}{N\mathcal{R}}, \tag{9}$$

where N_c is the number of atomic pairs in the translational unit cell. Here, $\mathcal{R} = 3$ if $(n_1 - n_2)/3N$ is integer and $\mathcal{R} = 1$ otherwise. We denote here this symmetry operation by $\mathbf{T}_a$ and it means translation along the tube axis by distance a. The translational unit cell consists then of a cylindrical tube of radius b and height a. The number of atoms in the unit cell is given by N_c.

To summarize, $\mathbf{C}_N$ is the symmetry operation of pure rotation (translations along the circumferential direction $\mathbf{c}$), $\mathbf{T}_a$ is the operation of pure translation, and $\mathbf{T}_h^\zeta$ is the (mixed) screw operation. It is worthy to mention that other symmetry operations were derived in [18] and [19] to fully characterize SWCNTs and MWCNTs. However, for the purpose of this paper, the previously mentioned three symmetry operations are enough to drive the basic mathematical form of the fields in the CNT environment. As will be shown in the next section, all other symmetry operations will alter only the number of terms taken in the resulted summations without changing the basic form.

4. GENERAL LINEAR PHENOMENOLOGICAL MODEL FOR THE ELECTROMAGNETIC FIELD INTERACTION WITH NANOTUBES

The main model we adopt to describe light-matter interaction in carbon nanotubes is given by the general susceptibility tensor $\overline{\overline{\chi}}$. Assuming that the external field is weak, it is possible to ignore nonlinear effects and write the polarization vector density as [22, 13]

$$\mathbf{P}\left(\mathbf{r},t\right) = \int_{t'} dt' \int_{\mathbf{r}'} d^3r' \overline{\overline{\chi}}\left(\mathbf{r},\mathbf{r}',t,t'\right) \cdot \mathbf{E}\left(\mathbf{r}',t'\right), \tag{10}$$

where $\mathbf{E}$ is the *total* microscopic electric field. We list below some of the important observations about the linear model in (10) that should be taken into consideration.

Before considering some of the general properties of this model, a clarification of the coordinate system that is chosen to represent

relation (**??**) is in order. As we view the CNT as a low-dimensional structure, the medium described by the susceptibility tensor $\overline{\overline{\chi}}$ above is defined only for observation points lying on the cylindrical surface of the nanotube. This means that *local* cylindrical coordinates should be employed, instead of the typical cylindrical coordinates used to describe the 3D space. That is, a point on a cylinder is described locally by φ and z. This allows us to write vectors located entirely on the cylinder surface. Strictly speaking, we consider a *curvilinear* coordinate system u, z, and φ, as shown in Figure 6. There, the two vectors traversed by z and φ are similar to those used to describe circular cylindrical geometrids. The reference direction for measuring the azimuthal direction is specified by the vector traversed by u. Thus, the CNT medium exists only at $u = b$, where b is the radius of the nanotube given by (3). Throughout this paper, we write any vector expressed in terms of this local coordinate system in the form $\mathbf{r} = \langle z, \varphi, u \rangle$.

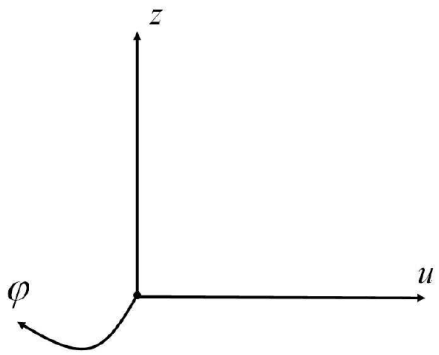

Figure 6. A local curvilinear coordinate system to describe the dynamics of carbon nanotubes. The z and φ correspond to the cylindrical variables, while u here is a chosen reference direction for the azimuthal vector traversed by φ.

Some of the general properties of the linear model in (10) can be summarized as follows.

(i) Since no effect can precede its cause, we must have $t' < t$.

(ii) According to relativity theory, no signal can travel faster than the speed of light c. Thus, we have the additional light cone causal condition $|\mathbf{r} - \mathbf{r}'| \leq c\,|t - t'|$.

(iii) Since the CNT atoms exist only on the tube surface $u = b$, $\mathbf{P}$ must vanish for any observation point outside the tube. Therefore, we write $\overline{\overline{\chi}} = 0$ for $u \neq b$.

(iv) Since $\mathbf{r}'$ is the field (source) point, this need not to be within the matter. Any point $\mathbf{r}'$ satisfying the relativistic criterion above must be taken into consideration. In others words, we have in general $\overline{\overline{\chi}} \neq 0$ for $u \neq b$ provided $|\mathbf{r} - \mathbf{r}'| \leq c\,|t - t'|$.

It is readily noticed from (10) that the susceptibility model is nonlocal or, equivalently, exhibits *spatial* dispersion. This is reflected in the fact that the dependence of χ on spacial variables is retained in the model. This will lead naturally to the interesting possibility of applying directly the symmetry group of the CNT, a task we achieve in the next section.

5. APPLICATION OF THE NANOTUBE SYMMETRY TO THE RESPONSE FUNCTION

Since $\overline{\overline{\chi}}(\mathbf{r}, \mathbf{r}', t, t')$ is a response function, it must obey the same symmetry operations of the CNT itself. The Bravais vector of an atom located on the CNT is given by

$$\mathbf{R}_{\mathbf{l}} = \langle z_{\mathbf{l}}, \varphi_{\mathbf{l}} \rangle, \tag{11}$$

where we remind the reader again that we are using local (Dupin) vectors. Here, $\mathbf{l} = (l_1, l_2)$ is a vector index enumerating the atomic position (l_1, l_2) on the CNT surface. $\varphi_{\mathbf{l}}$ and $z_{\mathbf{l}}$ are the φ- and z-locations of the $\mathbf{l}$th atom, respectively. The full microscopic structural information of the CNT can be taken into consideration by enforcing explicitly the symmetry group of CNTs. Therefore, by applying the symmetry operations $\mathbf{T}_a$ and $\mathbf{C}_N$, we find that the structure-preserving CNT displacements satisfy

$$\overline{\overline{\chi}}\left(z + l_1 a, \varphi + l_2 \frac{2\pi}{N}, z' + l_1 a, \varphi' + l_2 \frac{2\pi}{N}, u, u', t, t'\right) = \overline{\overline{\chi}}\left(\mathbf{r}, \mathbf{r}', t, t'\right), \tag{12}$$

where $l_{1,2} = 0, \pm 1, \pm 2, \ldots, \pm\infty$. Obviously, there is no periodicity in the radial direction. Equation (12) can be interpreted as the result of moving the primed and unprimed spatial coordinates according to the spatial symmetry operation of the CNT structure.

The mathematics of the coming parts can be simplified considerably if we re-write condition (12) above utilizing a different functional form for $\overline{\overline{\chi}}$. Namely, we have

$$\overline{\overline{\chi}}\left(z + l_1 a, \varphi + l_2 \frac{2\pi}{N}, u, \mathbf{r} - \mathbf{r}', t, t'\right) = \overline{\overline{\chi}}\left(\mathbf{r}, \mathbf{r} - \mathbf{r}', t, t'\right). \tag{13}$$

Therefore, from this equation we see that $\overline{\overline{\chi}}$ is (1) non-periodic in $\mathbf{r} - \mathbf{r}'$, (2) periodic with respect to z and φ, and (3) vanish for $u \neq b$.

By expanding (13) using Fourier series in the periodic arguments, observing meanwhile that the CNT "medium" exist only on the tube cylindrical surface, we find

$$\overline{\overline{\chi}}\left(\mathbf{r},\mathbf{r}-\mathbf{r}',t,t'\right)=\sum_{l_1=-\infty}^{\infty}\sum_{l_2=-\infty}^{\infty}\overline{\overline{\chi}}^{l_1,l_2}\left(\mathbf{r}-\mathbf{r}',t,t'\right)\delta\left(u-b\right)e^{jl_1N\varphi}e^{j\frac{2\pi}{a}l_2z}, \tag{14}$$

where $\overline{\overline{\chi}}^{l_1,l_2}$ are the (tensor) coefficients of the Fourier series expansion. The summations in (14) can be further simplified by applying the screw symmetry operation $\mathbf{T}_h^{\zeta}$ as follow

$$\overline{\overline{\chi}}\left(\mathbf{r},\mathbf{r}-\mathbf{r}',t,t'\right)=\overline{\overline{\chi}}\left(z-h,\varphi-\zeta,u,\mathbf{r}-\mathbf{r}',t,t'\right), \tag{15}$$

where ζ and h are the parameters of the screw operator defined in Section 3. Equations (14) and (15) give $\exp\left(-jl_1N\zeta-j\frac{2\pi}{a}l_2h\right)=1$, which translates to the following condition

$$\mathbf{C}:\ \ l_1N\zeta+l_2\frac{2\pi h}{a}=2\pi v,\ \ v=0,\pm1,\pm2,\ldots,\pm\infty. \tag{16}$$

In the next calculations, we write a summation over $\mathbf{l}=(l_1,l_2)$ that takes into consideration the condition (16) in the form $\sum_{\mathbf{l}|\mathbf{C}}$.

By applying the time symmetry condition (shift invariance), the final expression of the susceptibility can be written compactly as

$$\overline{\overline{\chi}}\left(\mathbf{r},\mathbf{r}-\mathbf{r}',t,t'\right)=\sum_{\mathbf{l}|\mathbf{C}}\overline{\overline{\chi}}^{\mathbf{l}}\left(\mathbf{r}-\mathbf{r}',t-t'\right)\delta\left(u-b\right)e^{jl_1N\varphi}e^{j\frac{2\pi}{a}l_2z}. \tag{17}$$

6. GENERAL EXPANSION FOR THE POLARIZATION DENSITY

Next, We expand the susceptibility tensor in the non-periodic arguments using Fourier integrals as follow

$$\begin{aligned}\overline{\overline{\chi}}\left(\mathbf{r},\mathbf{R},t,t'\right)\ =\ &\sum_{\mathbf{l}|\mathbf{C}}\int_{\mathbf{k}'}\int_{\omega'}\frac{d^3k'\,d\omega'}{\left(2\pi\right)^4}\overline{\overline{\chi}}^{\mathbf{l}}\left(\mathbf{k}',\omega'\right)\\&\times\delta\left(u-b\right)e^{j\frac{2\pi}{a}l_1z}e^{jNl_2\varphi}e^{j\,\mathbf{k}'\cdot\mathbf{R}}e^{j\omega'\tau},\end{aligned} \tag{18}$$

where $\mathbf{R}=\mathbf{r}-\mathbf{r}'$ and $\tau=t-t'$. The Fourier transform of the polarization density $\mathbf{P}$ is defined as

$$\mathbf{P}\left(\mathbf{k},\omega\right)=\int_{\mathbf{r}}\int_{t}d^3rdt\,\mathbf{P}\left(\mathbf{r},t\right)e^{-j\mathbf{k}\cdot\mathbf{r}}e^{-j\omega t}. \tag{19}$$

By using (18) and (10), Equation (19) gives

$$\mathbf{P}(\mathbf{k},\omega) = \int_{\mathbf{r}}\int_{t}\int_{\mathbf{R}}\int_{\tau} d^3r\,dt\,d^3R\,d\tau\, e^{-j\,\mathbf{k}\cdot\mathbf{r}} e^{-j\omega t} e^{j\frac{2\pi}{a}l_1 z} e^{jNl_2\varphi} e^{j\,\mathbf{k}'\cdot\mathbf{R}} e^{j\omega'\tau} \times \sum_{\mathbf{l}|\mathbf{C}} \int_{\mathbf{k}'}\int_{\omega'} \frac{d^3k'd\omega'}{(2\pi)^4} \overline{\overline{\chi}}^{\mathbf{l}}(\mathbf{k}',\omega')\,\delta(u-b)\cdot\mathbf{E}(\mathbf{r}-\mathbf{R},t-\tau), \quad (20)$$

where we have used the transformation $d^3Rd\tau = d(\mathbf{r}-\mathbf{r}')\,d(t-t') = d^3r'dt'$. By first performing the integration with respect to t, we have

$$\begin{aligned}\int_{t} dt\, e^{-j\omega t}\mathbf{E}(\mathbf{r}-\mathbf{R},t-\tau) &= e^{-j\omega\tau}\int_{\lambda} d\lambda\, e^{-j\omega\lambda}\mathbf{E}(\mathbf{r}-\mathbf{R},\lambda) \\ &= e^{-j\omega\tau}\mathbf{E}(\mathbf{r}-\mathbf{R},\omega), \end{aligned} \quad (21)$$

where the transformation $\lambda = t-\tau$ was used. Performing now the integration with respect to $\mathbf{r}$, it is possible to write

$$\begin{aligned}&\int_{\mathbf{r}} d^3r\, e^{-j\,\mathbf{k}\cdot\mathbf{r}}\mathbf{E}(\mathbf{r}-\mathbf{R},\omega)\,\delta(u-b)\,e^{j\frac{2\pi}{a}l_1 z}e^{jNl_2\varphi} \\ &= e^{-jk_u b}e^{-j(\mathbf{q}-\mathbf{g_l})\cdot\mathbf{R}}\mathbf{E}(\mathbf{q}-\mathbf{g_l},b,\omega) \end{aligned} \quad (22)$$

where with the transformation $\mathbf{s} = \mathbf{r}-\mathbf{R}$ was used. Here, $\mathbf{q} = \langle k_z, k_\varphi\rangle$ and the CNT reciprocal lattice vector $\mathbf{g_l}$ is given by

$$\mathbf{g_l} = \left\langle l_1\frac{2\pi}{a}, l_2N\right\rangle \quad (23)$$

Here, the Fourier transform can be computed as

$$\mathbf{E}(\mathbf{q},b,\omega) = \int_{-\infty}^{\infty}\int_{0}^{2\pi} bd\varphi\,dz\,\mathbf{E}(z,\varphi,u=b,\omega)\,e^{-j\mathbf{q}\cdot\mathbf{r}}. \quad (24)$$

Therefore, by substituting (21) and (22) into (20) we arrive to

$$\begin{aligned}\mathbf{P}(\mathbf{k},\omega) &= \int_{\mathbf{R}}\int_{\tau} d^3Rd\tau \sum_{\mathbf{l}|\mathbf{C}}\int_{\mathbf{k}'}\int_{\omega'} \frac{d^3k'd\omega'}{(2\pi)^4} e^{-j(\mathbf{q}-\mathbf{g_l}-\mathbf{k}')\cdot\mathbf{R}} e^{j(\omega'-\omega)\tau} \\ &\quad \times\overline{\overline{\chi}}^{\mathbf{l}}(\mathbf{k}',\omega')\cdot e^{-jk_u b}\mathbf{E}(\mathbf{q}-\mathbf{g_l},b,\omega), \end{aligned} \quad (25)$$

By using the sifting property of the Dirac delta function, it is possible to write

$$\int_{\mathbf{R}}\int_{\tau} d^3Rd\tau e^{-j(\mathbf{q}-\mathbf{g_l}-\mathbf{k}')\cdot\mathbf{R}} e^{j(\omega'-\omega)\tau} = (2\pi)^4\,\delta(\mathbf{q}-\mathbf{g_l}-\mathbf{k}')\,\delta(\omega'-\omega). \quad (26)$$

Plugging this integral into (25), we get

$$\mathbf{P}(\mathbf{k},\omega) = \sum_{\mathbf{l}|\mathbf{C}} \int_{\mathbf{k}'} \int_{\omega'} d^3k' d\omega' \delta(\mathbf{q}-\mathbf{g}_{\mathbf{l}}-\mathbf{k}') \delta(\omega'-\omega) \times \overline{\overline{\chi}}^{\mathbf{l}}(\mathbf{k}',\omega') \cdot e^{-jk_u b} \mathbf{E}(\mathbf{q}-\mathbf{g}_{\mathbf{l}},b,\omega). \quad (27)$$

Using the sifting property again, the integrations with respect to $\mathbf{k}'$ and ω' simplifies to single evaluations and finally we obtain

$$\mathbf{P}(\mathbf{k},\omega) = \sum_{\mathbf{l}|\mathbf{C}} \overline{\overline{\chi}}^{\mathbf{l}}(\mathbf{q}-\mathbf{g}_{\mathbf{l}},\omega) \cdot e^{-jk_u b} \mathbf{E}(\mathbf{q}-\mathbf{g}_{\mathbf{l}},b,\omega). \quad (28)$$

Thus, this key results tells us that the polarization $\mathbf{P}$ of the CNT induced by a field with spatial frequency $\mathbf{q}$ and temporal frequency ω appears as a function of the same temporal frequency but contains, in addition to the $\mathbf{q}$-component, an infinite set of harmonics of $\mathbf{g}_{\mathbf{l}}$, which are defined by (23). The spectral description of the electromagnetic interaction with nanotubes, which are viewed as low-dimensional structures, takes this simple form depicted in (28) because of the convenience of working with the local coordinate system introduced in Figure 6.

7. EIGENMODE EXCITATION OF THE NANOTUBE MEDIUM

To understand the physical meaning of Equation (28), let us assume that there is an eigenfunction wave mode impinging on the CNT medium given by

$$\mathbf{E}(\mathbf{r},t) = \mathbf{E}^0 e^{-j\,\mathbf{k}_0\cdot\mathbf{r}} e^{j\omega_0 t}, \quad (29)$$

where $\mathbf{k}_0 = \langle k_{z0}, k_{\varphi 0}, k_{u0}\rangle$. Its Fourier transform, evaluated using (24), is given by

$$\mathbf{E}(\mathbf{k},b,\omega) = \int_{\mathbf{r}} \int_{\omega} d^2r\, dt\, \mathbf{E}^0 e^{-jk_{u0}b} e^{-j\mathbf{q}_0\cdot\mathbf{r}} e^{j\omega_0 t} e^{-j\,\mathbf{q}\cdot\mathbf{r}} e^{-j\omega t} = (2\pi)^4 \mathbf{E}^0 e^{-jk_{u0}b} \delta(\mathbf{q}+\mathbf{q}_0)\delta(\omega-\omega_0) \quad (30)$$

where $\mathbf{q}_0 = \langle k_{z0}, k_{\varphi 0}\rangle$. Therefore, substituting (30) into Equation (28) we get

$$\mathbf{P}(\mathbf{k},\omega) = (2\pi)^4 \mathbf{E}^0 e^{-j(k_u+k_{u0})b} \sum_{\mathbf{l}|\mathbf{C}} \overline{\overline{\chi}}^{\mathbf{l}}(\mathbf{q}-\mathbf{g}_{\mathbf{l}},\omega)\delta(\mathbf{q}-\mathbf{g}_{\mathbf{l}}+\mathbf{q}_0)\delta(\omega-\omega_0). \quad (31)$$

Calculating now the inverse Fourier transform, we find

$$\begin{aligned}\mathbf{P}(\mathbf{r},t) &= \frac{1}{(2\pi)^4}\int\limits_{\mathbf{k}}\int\limits_{\omega} d^3k\, d\omega\, \mathbf{P}(\mathbf{k},\omega)\, e^{j\mathbf{k}\cdot\mathbf{r}} e^{j\omega t} \\ &= \mathbf{E}^0 \int\limits_{\mathbf{k}}\int\limits_{\omega} d^3k\, d\omega\, e^{-j(k_u+k_{u0})b} \sum_{\mathbf{n}|\mathbf{C}} \overline{\overline{\chi}}^{\mathbf{l}}(\mathbf{q}-\mathbf{g}_{\mathbf{l}},\omega) \\ &\quad \times\delta(\mathbf{q}-\mathbf{g}_{\mathbf{l}}+\mathbf{q}_0)\,\delta(\omega-\omega_0)\, e^{j\mathbf{k}\cdot\mathbf{r}} e^{j\omega t}. \end{aligned} \tag{32}$$

By evaluating the integrals, the final answer can be written in the following compact form

$$\mathbf{P}(\mathbf{r},t) = \mathbf{E}^0 \left[\sum_{\mathbf{l}|\mathbf{C}} \overline{\overline{\chi}}^{\mathbf{l}}(-\mathbf{q}_0,\omega_0)\ \delta(u-b)\, e^{-jk_{u0}b}\, e^{j\mathbf{g}_{\mathbf{l}}\cdot\mathbf{r}}\right]\ e^{-j\mathbf{q}_0\cdot\mathbf{r}} e^{j\omega_0 t}. \tag{33}$$

The term between the brackets in Equation (33) has the form of a Fourier series, and thus it represents a periodic function with a period $\mathbf{R}_{\mathbf{l}}$, i.e., the fundamental lattice vector. Therefore, the form of the induced polarization given in (33) can be easily interpreted as a Bloch theorem adapted to the lower-dimensional structure of the nanotube.

From the linearity of Maxwell's equations (superposition), it is readily established that the field response to the polarization density (33) can be expanded as

$$\mathbf{E}(\mathbf{r},t) = \sum_{\mathbf{l}|\mathbf{C}} T\,\overline{\overline{\chi}}^{\mathbf{l}}(-\mathbf{q}_0,\omega_0)\cdot\mathbf{E}^0\delta(u-b)\, e^{-jk_{u0}b} e^{j\mathbf{g}_{\mathbf{l}}\cdot\mathbf{r}} e^{-j\mathbf{q}_0\cdot\mathbf{r}} e^{j\omega_0 t}, \tag{34}$$

where T is to the radiation operator that relates the polarization to the field induced in the CNT medium. An explicit expression for this operator will be derived in the next section.

Equation (34) shows again that the response of the CNT to an eigenmode excitation is a new wave consisting of the spatial and temporal frequencies of the original mode, plus higher-order Floquet modes at harmonics of the reciprocal lattice vector. Direct averaging of the field may lead to removing the fast-varying components of (34). This means that the microscopic information, the mathematical solution which is truly satisfying the symmetry group of the structure, will be lost. For the determination of the optical and electrical characteristics of materials starting from the atomic model, it is exactly such rapid variations what constitute the *local* field acting on the medium particles [8, 9, 13, 15, 22]. Therefore, for a complete electrodynamic theory for CNTs, the full field in (34) must be used without direct averaging.

8. BOUNDARY-VALUE PROBLEM FORMULATION FOR THE ELECTRODYNAMICS OF NANOTUBES

Assume an environment consisting of a single CNT surrounded by free space. Our goal is to formulate the suitable boundary-value problem of the electromagnetic field interaction with this environment. Let us assume first that there is an external incident field given by $(\mathbf{E}^{\text{inc}}, \mathbf{H}^{\text{inc}})$, which can be microscopic or macroscopic[†], and are propagating in an infinite and homogenous (free) space. The incident field will produce an induced fields $\left(\mathbf{E}^{\text{ind}}, \mathbf{H}^{\text{ind}}\right)$ because of the perturbation caused by the existence of the CNT in free space. The total field is given by

$$\mathbf{E} = \mathbf{E}^{\text{ind}} + \mathbf{E}^{\text{inc}}, \;\; \mathbf{H} = \mathbf{H}^{\text{ind}} + \mathbf{H}^{\text{inc}}. \tag{35}$$

Equation (10) connects the polarization density of the medium with the total field. Since only linear operators are considered here, the medium response will split into two parts satisfying

$$\mathbf{P} = \mathbf{P}^{\text{ind}} + \mathbf{P}^{\text{inc}}, \tag{36}$$

where we have

$$\mathbf{P}^{\text{inc}}(\mathbf{r},t) = \int\limits_{t'} dt' \int\limits_{\mathbf{r}'} d^3r' \, \overline{\overline{\chi}}(\mathbf{r}, \mathbf{r}', t, t') \cdot \mathbf{E}^{\text{inc}}(\mathbf{r}', t') \tag{37}$$

and

$$\mathbf{P}^{\text{ind}}(\mathbf{r},t) = \int\limits_{t'} dt' \int\limits_{\mathbf{r}'} d^3r' \, \overline{\overline{\chi}}(\mathbf{r}, \mathbf{r}', t, t') \cdot \mathbf{E}^{\text{ind}}(\mathbf{r}', t'). \tag{38}$$

The polarization density is connected to the current by [9]

$$\mathbf{J} = \frac{\partial \mathbf{P}}{\partial t}. \tag{39}$$

By combining the two curl Maxwell's equations together with (35)–(39) and arranging the resulted terms, we arrive to the following equations

$$\nabla \times \mathbf{H}^{\text{ind}}(\mathbf{r}, t) = \varepsilon_0 \frac{\partial \mathbf{E}^{\text{ind}}(\mathbf{r}, t)}{\partial t} + \mathbf{J}_{\text{eq}}(\mathbf{r}, t) \tag{40}$$

and

$$\nabla \times \mathbf{E}^{\text{ind}}(\mathbf{r}, t) = -\mu_0 \frac{\partial \mathbf{H}^{\text{ind}}(\mathbf{r}, t)}{\partial t}, \tag{41}$$

[†] The theory developed here is general enough to handle both cases.

where the equivalent electric current is given by

$$\mathbf{J}_{\text{eq}}(\mathbf{r},t)=\frac{\partial}{\partial t}\int\limits_{t'}dt'\int\limits_{\mathbf{r}'}d^3r'\overline{\overline{\chi}}\left(\mathbf{r},\mathbf{r}',t,t'\right)\cdot\left[\mathbf{E}^{\text{inc}}\left(\mathbf{r}',t'\right)+\mathbf{E}^{\text{ind}}\left(\mathbf{r}',t'\right)\right]. \tag{42}$$

Equations (40) and (41), together with $\nabla\cdot\mathbf{D}=\rho_{\text{ex}}$ and $\nabla\cdot\mathbf{B}=0$, where ρ_{ex} is the external charge, represent a complete time-domain boundary-value problem for the electrodynamics in the CNT environment that takes into consideration the microscopic nature of the nanotube. Moreover, by assuming that an accurate quantum-mechanical solution was used for the susceptibility tensor $\overline{\overline{\chi}}$ in (42), this formulation for the electrodynamics of the nanotube can be considered semi-classically exact.

By invoking the field decomposition (35), the system of equations (40) and (41) can be solved to provide the induced field as the response to the incident field as given by the following expression

$$\mathbf{E}^{\text{ind}}=\left[-\frac{\partial^2}{\partial t^2}\left(\frac{1}{c^2}+\Im\right)+\nabla\times\nabla\times\right]^{-1}\frac{\partial^2}{\partial t^2}\Im\mathbf{E}^{\text{inc}}, \tag{43}$$

where the action of the operator $\Im$ when applied to a field $\mathbf{F}$ is defined by

$$\Im\mathbf{F}=-\mu_0\int\limits_{t'}dt'\int\limits_{\mathbf{r}'}d^3r'\overline{\overline{\chi}}\left(\mathbf{r},\mathbf{r}',t,t'\right)\cdot\mathbf{F}\left(\mathbf{r}',t'\right). \tag{44}$$

By using (37), it follows that $\mathbf{P}^{\text{inc}}=(-1/\mu_0)\,\Im\mathbf{E}^{\text{ind}}$. Therefore, from (43), we arrive to the following expression for the radiation operator T in the relation $\mathbf{E}^{\text{ind}}=T\mathbf{P}^{\text{inc}}$

$$T=-\mu_0\left[-\frac{\partial^2}{\partial t^2}\left(\frac{1}{c^2}+\Im\right)+\nabla\times\nabla\times\right]^{-1}\frac{\partial^2}{\partial t^2}. \tag{45}$$

On the other hand, it is also possible to express Maxwell's equations directly in the spectral domain. In this case, we apply the Fourier transform to (40) and (41), making use of (28) to expand (38), arriving to the following equations

$$\mathbf{k}\times\mathbf{H}^{\text{ind}}\left(\mathbf{k},\omega\right)=\omega\varepsilon_0\mathbf{E}^{\text{ind}}\left(\mathbf{k},\omega\right)+\mathbf{J}_{\text{eq}}\left(\mathbf{k},\omega\right) \tag{46}$$

and

$$\mathbf{k}\times\mathbf{E}^{\text{ind}}\left(\mathbf{k},\omega\right)=-\omega\mu_0\mathbf{H}^{\text{ind}}\left(\mathbf{k},\omega\right), \tag{47}$$

where

$$\mathbf{J}_{\mathrm{eq}}(\mathbf{k},\omega) = \omega \sum_{\mathbf{l}|\mathbf{C}} \overline{\overline{\chi}}^{\mathbf{l}}(\mathbf{q}-\mathbf{g}_{\mathbf{l}},\omega)\cdot e^{-jk_u b} \times \left[\mathbf{E}^{\mathrm{inc}}(\mathbf{q}-\mathbf{g}_{\mathbf{l}},b,\omega)+\mathbf{E}^{\mathrm{ind}}(\mathbf{q}-\mathbf{g}_{\mathbf{l}},b,\omega)\right]. \quad (48)$$

It is worthy to mention that if the source is at infinity, then the incident field takes the simple form of plane wave. This allows for further simplification in the current of (42) if the expansion (34) is taken into account.

Equations (40) and (41) can be readily discretized using differential solvers, like Finite-Element Method (FEM) or Finite Difference Time-Domain Method (FDTD), which take advantage of the fact that the problem is set most generally in the time domain. Alternatively, one can exploit the equivalent currents of (42) to write spectral domain integral equations and solve them using the Method of Moment (MoM). Such direct numerical solutions are not attempted in this paper.

9. GREEN'S FUNCTIONS FOR CARBON NANOTUBES

The general microscopic expansion of the fields formulated previously can be used to derive the Green's functions of the CNT located in infinite homogenous environment. Such derivation is not based on the traditional boundary condition formulation familiar in electromagnetics [10, 11]. The motivation of the current work is the fact, established formally in the previous parts, that at the nanoscale level, the microscopic details of the spatial nonlocality should be fully taken into consideration [10]. Besides their theoretical importance, the Green's functions can be utilized to build a fast and efficient general Method of Moment code to compute both the CNT near- and far-fields.

Consider a point source lying outside the CNT as shown in Figure 7. The source radiates a wave that interacts with the CNT surface. The result of this interaction is three different waves. One is propagating along the nanotube surface and we call it the *refracted* wave. Another wave is transmitted inside the tube, called here *trapped* or *transmitted* field. The third part is reflected back and is duped *diffracted*[‡].

[‡] We refer here to 'diffraction' instead of "reflection" because, in contrast to the macroscopic case, there is no meaning for 'continuous surface' upon which the wave is reflected. The term 'diffraction' from individual atoms seems more convenient for a microscopic theory of light-matter interaction.

The incident wave interacts with the CNT medium, producing the polarization given by (28), which, according to the linear model of Section 4, is nonzero only on the nanotube cylindrical surface. This polarization, in turn, will radiate everywhere. We write the radiation operator responsible of transforming the induced polarization into refracted, trapped, and diffracted fields as T_r, T_t, and T_d, respectively. Those operators can be found by solving the boundary-value problem of (40)–(42). In the following parts, a time-harmonic dependence of the form $\exp(j\omega t)$ is assumed and suppressed everywhere.

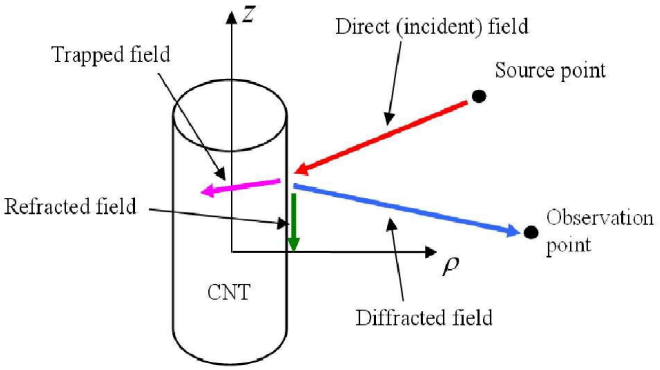

Figure 7. Source and observation points located outside the CNT. The point source radiates a direct wave that interacts with the CNT and results in refracted, trapped, and diffracted fields.

Let the source be an electric current located at the position $\mathbf{r}'$ and given by

$$\mathbf{J}(\mathbf{r}') = \hat{v}\delta(\mathbf{r} - \mathbf{r}'), \tag{49}$$

where $\hat{v}$ is a unit vector specifying the direction of the current. The electric field radiated by this source is given by [10]

$$\mathbf{E}(\mathbf{r}) = -j\omega\mu \int d^3r' \, \bar{\mathbf{G}}(\mathbf{r}, \mathbf{r}') \cdot \mathbf{J}(\mathbf{r}'), \tag{50}$$

where we have assumed that the source environment is an infinite homogeneous space, with characteristics (ε, μ) (i.e., remove the CNT from the source environment). The Dyadic Green's functions of free space can be written as [10]

$$\bar{\mathbf{G}}(\mathbf{r}, \mathbf{r}') = \left[\bar{\mathbf{I}} + \frac{\nabla'\nabla'}{k^2}\right] g(\mathbf{r}, \mathbf{r}'), \tag{51}$$

where $\bar{\mathbf{I}}$ is the identity dyad, $k = \omega\sqrt{\varepsilon\mu}$ is the free space wavenumber, and $g(\mathbf{r}, \mathbf{r}')$ is the scalar Green's function given by

$$g(\mathbf{r}, \mathbf{r}') = \frac{e^{-jk|\mathbf{r}-\mathbf{r}'|}}{4\pi|\mathbf{r}-\mathbf{r}'|}, \tag{52}$$

By substituting (49), (51), and (52) into (50), the incident field is simplified to

$$\mathbf{E}^{\text{inc}}(\mathbf{r}) = -j\omega\mu\left[\bar{\mathbf{I}} + \frac{\nabla'\nabla'}{k^2}\right] \cdot \hat{v}\frac{e^{-jk|\mathbf{r}-\mathbf{r}'|}}{4\pi|\mathbf{r}-\mathbf{r}'|}. \tag{53}$$

We will make use of the following form of Sommerfeld identify [10]

$$\frac{e^{-jk|\mathbf{r}-\mathbf{r}'|}}{|\mathbf{r}-\mathbf{r}'|} = -j\int_0^\infty dk_\rho \frac{k_\rho}{k_z} e^{-jk_z(z-z')} J_0\left(k_\rho|\rho-\rho'|\right), \tag{54}$$

where

$$k_z = \sqrt{k^2 - k_\rho^2} \tag{55}$$

and J_0 is the Bessel function of the first kind. Then, equation (53) can be written as

$$\mathbf{E}^{\text{inc}}(\mathbf{r}) = \mathbf{D}'\int_0^\infty dk_\rho \frac{k_\rho}{k_z} e^{-jk_z(z-z')} J_0\left(k_\rho|\rho-\rho'|\right), \tag{56}$$

where the differential operator $\mathbf{D}'$ is given by

$$\mathbf{D}' = -\frac{\omega\mu}{4\pi}\left[\bar{\mathbf{I}} + \frac{\nabla'\nabla'}{k^2}\right] \cdot \hat{v}. \tag{57}$$

Moreover, from the time-harmonic assumption and the particular expansion of the field in (56) we have

$$\nabla' = \hat{z}jk_z + \hat{\varphi}'\frac{jn}{\rho'} + \hat{\rho}'\frac{\partial}{\partial\rho'}. \tag{58}$$

By utilizing the addition theorem [10, 25], it is possible to expand the Bessel function of (56) in cylindrical harmonics as follow

$$J_0\left(k_\rho|\rho-\rho'|\right) = \sum_{n=-\infty}^{\infty} J_n\left(k_\rho\rho'\right) J_n\left(k_\rho\rho\right) e^{-jn(\varphi-\varphi')}. \tag{59}$$

Therefore, the primary field in (56) becomes

$$\mathbf{E}^{\text{inc}}(\mathbf{r}) = \mathbf{D}' \sum_{n=-\infty}^{\infty} \int_0^{\infty} dk_\rho \frac{k_\rho}{k_z} J_n(k_\rho \rho') J_n(k_\rho \rho) e^{-jn(\varphi-\varphi')} e^{-jk_z(z-z')}. \tag{60}$$

This means that the field radiated by a point source can be written as a sum of plane waves in the transverse direction and cylindrical wave in the radial direction.

According to (60), the point source will radiate a continuum of plane waves in both the transverse and radial directions. By identifying the cylindrical coordinates z and φ with those in the local coordinate system in Figure 6, the eigenfunction wave mode impinging on the CNT can be expressed as

$$J_n(k_\rho \rho) e^{-jk_z z - jn\varphi} = J_n(k_\rho \rho) e^{-j\,\mathbf{q}_0 \cdot \mathbf{r}}, \tag{61}$$

where

$$\mathbf{q}_0 = \langle k_z, n \rangle. \tag{62}$$

We expand now the cylindrical wave function $J_n(k_\rho \rho)$ using the following integral representation [12, 25]

$$J_n(k_\rho \rho) = \frac{j^{-n}}{2\pi} \int_0^{2\pi} d\alpha e^{jn\alpha} e^{jk_\rho \cos\alpha \rho}. \tag{63}$$

This integral representation can be interpreted in two equivalent ways. First, it may be taken to represent the cylindrical wave function $J_n(k_\rho \rho)$ as a superposition of plane waves, all with the same wavenumber k_ρ, but propagating in the directions $u(\alpha) = \rho \cos\alpha$. The second interpretation is that those plane waves have varying wavenumbers given by $k(\alpha) = k_\rho \cos\alpha$ but with fixed (arbitrary) spatial direction ρ. If we take the second interpretation, we can assume that the reference spatial direction coincides with our coordinate u in the local system of Figure 6. Therefore, the wave in (61) can be written as

$$J_n(k_\rho u) e^{-j\mathbf{q}_0 \cdot \mathbf{r}} = \frac{j^{-n}}{2\pi} \int_0^{2\pi} \left(d\alpha e^{jn\alpha} \right) e^{-j\mathbf{q}_0 \cdot \mathbf{r} - jk'_\rho(\alpha) u}, \tag{64}$$

where

$$k'_\rho(\alpha) = -k_\rho \cos\alpha. \tag{65}$$

According to the key result (34), the microscopic field generated by the eigenmode $e^{-j\mathbf{q}_0\cdot\mathbf{r}-jk'_\rho u}$ takes the form

$$\sum_{l_1,l_2|\mathbf{C}} T_{r,t,d}\overline{\overline{\chi}}^{\mathbf{l}}\left(-\mathbf{q}_0\right)\cdot\mathbf{D}'e^{-jk'_\rho b}\delta\left(u-b\right)e^{j\frac{2\pi}{a}l_1 z}e^{jNl_2\varphi}\,e^{-j\,\mathbf{q}_0\cdot\mathbf{r}}$$
$$=\sum_{l_1,l_2|\mathbf{C}} T_{r,t,d}\overline{\overline{\chi}}^{\mathbf{l}}\left(-\mathbf{q}_0\right)\cdot\mathbf{D}'e^{-jk'_\rho b}\delta\left(u-b\right)e^{j\left(\frac{2\pi}{a}l_1-k_z\right)z}e^{j(Nl_2-n)\varphi}. \quad (66)$$

By using (61) and (66) in (56), the total electric Green's functions can be calculated by superposition. We have

$$\mathbf{G}^e_{r,t,d}\left(\mathbf{r},\mathbf{r}'\right)=\mathbf{E}^{\text{inc}}+\sum_{n=-\infty}^{\infty}\sum_{l_1|\mathbf{C}}\sum_{l_2|\mathbf{C}}\left\{\int_{-\infty}^{\infty}\int_{0}^{2\pi}d\alpha dk_\rho\frac{j^{-n}}{2\pi}\frac{k_\rho}{k_z}\right.$$
$$\times T_{r,t,d}\overline{\overline{\chi}}^{\mathbf{l}}\left(-\mathbf{q}_0\right)\cdot\mathbf{D}'J_n\left(k_\rho\rho'\right)e^{-jk_\rho b\cos\alpha}\delta\left(u-b\right)e^{jn\varphi'}e^{jk_z z'}$$
$$\left.\times\, e^{jn\alpha}e^{j\left(\frac{2\pi}{a}l_1-k_z\right)z}e^{j(Nl_2-n)\varphi}\right\} \quad (67)$$

The magnetic Green's functions follows directly from Maxwell's equations and are given by

$$\mathbf{G}^h_{r,t,d}\left(\mathbf{r},\mathbf{r}'\right)=\frac{1}{-j\omega\mu_0}\nabla\times\mathbf{G}^e_{r,t,d}\left(\mathbf{r},\mathbf{r}'\right). \quad (68)$$

Because of the choice of the Sommerfeld integral adopted by (54), no modification is needed for the case when the source is inside the CNT. However, while evaluating the integral with respect to k_ρ, caution must be taken to avoid passing over the pole and branch point singularities of the integrand.

The apparent complexity of (67), compared with other problems in conventional engineering electromagnetics, is a natural consequence of the microscopic model introduced in Section 4. This is a price that must be paid for the abundance of the much simpler, but arguably potentially problematic, program of macroscopic Maxwell's equation[§].

10. CONCLUSION

In this paper, a formalism for the electrodynamics of carbon nanotubes was proposed. A general nonlocal linear phenomenological model

[§] For applications where the far-field response is the parameter of interest, the higher-order Floquet modes in the z-direction can be ignored, which amounts to a simple averaging operation applied to the Green's function in (67), removing hence the l_1 spatial modes.

was assumed in the study of the problem of the interaction of low-dimensional structure with electromagnetic fields. The symmetry group of the structure was employed to obtain the Bloch form of the spectral properties of the interaction. The derived expressions are then used to highlight a methodology for the computation of the Green's functions of the nanotube.

ACKNOWLEDGMENT

This work was partially supported by the Department of Electrical Engineering, University of Mississippi and the National Science Foundation under Grant No. ECS-524293. Also, partial support for this research was provided by ONR Grant # N00014-07-1-1010, Office of Naval Research, Solid Mechanics Program (Dr. Yapa D.S. Rajapakse, Program Manager).

REFERENCES

1. Poole, C. P. and F. J. Owens, *Introduction to Nanotechnology*, Wiley-Interscience, 2003.
2. Kong, F., K. Li, B.-I. Wu, H. Huang, H. Chen, and J. A. Kong, "Propagation properties of the SPP modes in nanoscale narrow metallic gap, channel, and hole geometries," *Progress In Electromagnetics Research*, PIER 76, 449–466, 2007.
3. Talele, K. and D. S. Patil, "Analysis of wave function, energy and transmission coefficients in GaN/ALGaN superlattice nanostructures," *Progress In Electromagnetics Research*, PIER 81, 237–252, 2008.
4. Iijima, S., "Helical microtabules of graphitic carbon," *Nature*, Vol. 354, 56–58, 1991.
5. Anantram, M. and F. Leonard, "Physics of carbon nanotube electronic devices," *Reports on Progress in Physics*, Vol. 69, 507–561, February 2006.
6. Smalley, R. E., M. S. Dresselhaus, G. Dresselhaus, and P. Avouris, *Carbon Nanotubes: Synthesis, Structure, Properties and Applications*, Springer, 2001.
7. Mikki, S. M. and A. A. Kishk, "Exact derivation of the dyadic Green's functions of carbon nanotubes using microscopic theory," *International IEEE APS Symposium*, Hawaii, June 2007.
8. Wooten, F., *Optical Properties of Solids*, Academic Press, 1972.
9. Jackson, J. D., *Classical Electrodynamics*, 3rd edition, John Wiley & Sons, 1999.

10. Chew, W. C., *Waves and Fields in Inhomogeneous Media*, re-print edition, IEEE Press, 1999.
11. Balanis, C., *Advanced Engineering Electromagnetics*, John Wiley & Sons, 1989.
12. Stratton, J., *Electromagnetic Theory*, McGraw-Hill, 1941.
13. Toyozawa, Y., *Optical Processes in Solids*, Cambridge University Press, 2003.
14. Brillouin, L., *Wave Propagation in Periodic Structures*, 1956.
15. Born, M. and K. Haung, *Dynamical Theory of Crystal Lattices*, 1st edition, Oxford University Press, London, 1954.
16. Grosso, G. and G. Parravicini, *Solid-State Physics*, Academic Press, 2000.
17. White, C. T., D. H. Robertson, and J. W. Mintmire, "Helical and rotational symmetries of nanoscale graphitic tubules," *Phys. Rev. B*, Vol. 47, No. 9, 5485–5488, March 1993.
18. Damnjanovic, M., I. Milosevic, T. Vukovic, and R. Sredanovic, "Full-symmetry, optical activity, and potentials of single-wall and multi-wall nanotubes," *Phys. Rev. B*, Vol. 60, No. 4, 2728–2739, July 1999.
19. Damnjanovic, M., I. Milosevic, T. Vukovic, and R. Sredanovic, "Symmetry and lattices of single-wall nanotubes," *J. Phys. A*, Vol. 32, 4097–4104, 1999.
20. Cohen-Tannoudjii, C., J. Dupont-Roc, and G. Grynberg, *Photons and Atoms: Introduction to Quantum Electrodynamics*, Wiley, 1989.
21. Pekar, S. I., "Theory of electromagnetic waves in a crystal in which excitons are produced," *Sov. Phys. JETP*, Vol. 6, 785, 1957.
22. Agranovich, V. M. and V. L Ginsburg, *Crystal Optics and Spatial Dispersion, and Excitons*, Springer, 1984.
23. Halevi, P. (ed.), *Spatial Dispersion in Solids and Plasmas*, Springer, 1992.
24. Cho, K., "Nonlocal theory of radiation-matter interaction: Boundary-condition-less treatment of Maxwell equations," *Prog. Theor. Phys. Suppl.*, No. 106, 225–233, 1991.
25. Abramowitz, M. and I. A. Stegun, *Handbook of Mathematical Functions*, Dover Publications, 1965.